A terahertz plasmon cavity detector

G. C. Dyer,[1,a)] N. Q. Vinh,[1] S. J. Allen,[1] G. R. Aizin,[2] J. Mikalopas,[2] J. L. Reno,[3] and E. A. Shaner[3]
[1]*Institute for Terahertz Science and Technology, UC Santa Barbara, Santa Barbara, California 93106, USA*
[2]*Kingsborough College, The City University of New York, Brooklyn, New York 11235, USA*
[3]*Sandia National Laboratories, P.O. Box 5800, Albuquerque, New Mexico 87185, USA*

(Received 22 July 2010; accepted 1 October 2010; published online 10 November 2010)

Sensitivity of a plasmonic detector is enhanced by integrating a broadband log-periodic antenna with a two-dimensional plasma cavity that is defined by source, drain, and multiple gates of a GaAs/AlGaAs high electron mobility transistor. Both narrow-band terahertz detection and a rich harmonic spectrum are evident. With a bolometric sensor in the channel, we report responsivity, on resonance at 235–240 GHz and at 20 K, of up to 7 kV/W and a noise equivalent power of 5×10^{-10} W/Hz$^{1/2}$. © *2010 American Institute of Physics*. [doi:10.1063/1.3513339]

Recent research has yielded myriad advances in terahertz (THz) detector technology[1–6] but narrow-band, electronically tunable THz detection with high sensitivity has not yet been fully realized. Resonant absorption by two-dimensional (2D) plasmons presents an avenue to achieve this important capability. Sufficiently sensitive detectors would make possible THz spectroscopic single-point elements and imaging arrays. 2D plasmons in both Si metal-oxide-semiconductor field-effect transistors and III–V semiconductor heterostructures have long been exploited to establish a resonant mechanism to sense THz radiation in a solid-state device.[7–11] Previous work by Shaner *et al.* used a relatively large area grating coupler to excite 2D THz plasmons in a GaAs/AlGaAs high electron mobility transistor (HEMT) and subsequently enhanced the detector signal by integrating a bolometric sensor[12,13] and by mounting the detector on a thin membrane.[14] In this letter, we describe a plasmonic detector in which the grating coupler is replaced by a micron scale plasmonic cavity with a bolometric sensor at the vertex of a log periodic antenna. Excitation of 2D plasmons in short-channel HEMT structures was recently used for THz detection by Knap *et al.*[15] However, our device implementation is fundamentally different. The responsivity of the devices discussed in this letter is enhanced three orders of magnitude over previous detectors with grating couplers; the sensitivity and response time are approaching the requirements of a focal plane array for video rate spectroscopic THz imaging.

The detector (Fig. 1) was fabricated from a double quantum well GaAs/AlGaAs heterostructure (Sandia wafer EA1149) with a total electron density of 4.14×10^{11} cm^{-2}, a low temperature mobility of $\sim 10^6$ cm^2/V s and gate pinch off voltage of $V_{TH}=-2.4$ V. The quantum wells are 400 nm below the surface, 20 nm thick, and spaced 7 nm from each other. A 14 μm long by 10 μm wide channel is defined by a mesa etch and the source and drain Ohmic contacts. After three 2 μm wide gates spaced from neighboring terminals by 2 μm are fabricated, a 1.5 mm diameter broadband log-periodic antenna is overlaid on top of the annealed GeAu source and drain contacts. A similar design of a three gate plasmonic detector was theoretically considered by Ryzhii *et al.*[16] The antenna couples radiation polarized parallel to the current flow in the HEMT. The gate labeled barrier gate (BG) is biased beyond threshold and the pinched off channel serves as an integrated bolometric sensor.[12] Due to the depletion of the channel below the BG, 2D plasma cavities are formed between source and BG and BG and drain. The effective electron density in each cavity can be modulated by the source gate (SG) and drain gate (DG), respectively.

The detector response as a function of frequency and bias point has been characterized using the UCSB free electron laser (FEL) as a pulsed THz source. The multigate transistor is operated at 20 K with BG biased beyond depletion to $V_{BG}=-2.5$ V and drain current set to $I_{SD}=+500$ nA such that carriers are drifting from source toward the bolometric element. Thus the detector is preferentially sensitive to carriers heated in the cavity between source and BG, and bias applied to the SG tunes the 2D plasma resonance in the source-side cavity. For a fixed bias current, the detector signal is measured as the change in source-drain voltage, δV_{SD}. The signal is converted to responsivity using an absolute power meter to determine incident power. The response, shown in Fig. 2, is not corrected for losses in the window and any beam/detector cross section mismatch.

With 420 GHz excitation, two plasmon cavity modes are evident with peaks at gate biases of approximately $V_{SG}=-0.7$ V and $V_{SG}=-1.8$ V. When the THz excitation is tuned to 480 GHz, these two modes shift to approximately $V_{SG}=0$ V and $V_{SG}=-1.4$ V, respectively, while an addi-

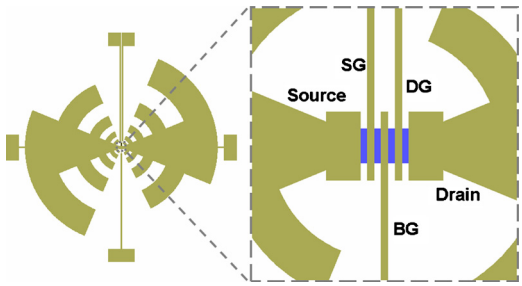

FIG. 1. (Color online) Device layout. The log-periodic antenna is 1.5 mm in diameter (left). The detector is located at the vertex of the antenna, and consists of a multigate HEMT with a 14 μm long, 10 μm wide channel (right, highlighted in blue). Plasmonic cavities are formed between the BG and source contact and BG and drain contact. All gates are 2 μm in width.

a)Electronic mail: gdyer@physics.ucsb.edu.

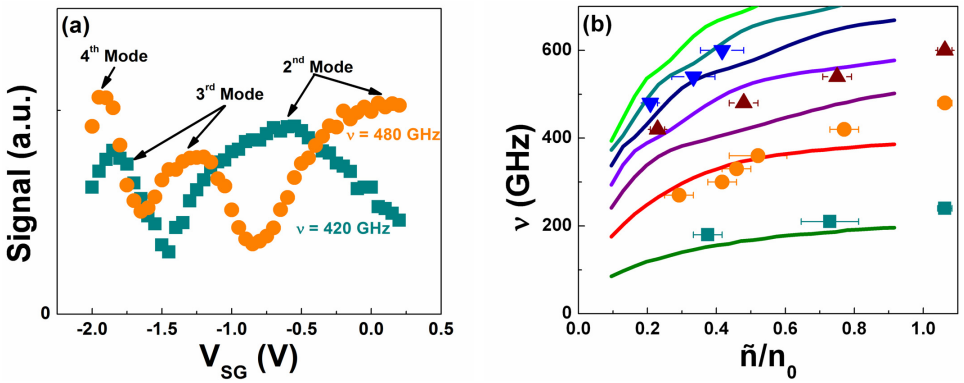

FIG. 2. (Color online) (a) Detector signal with incident radiation tuned to 420 GHz (squares), 480 GHz (circles). Higher order plasmon modes are evident as the source gate voltage is tuned. The detector is operated at T=20 K, I_{SD}=500 nA, and V_{BG}=−2.5 V. (b) Four experimentally measured plasmon modes (squares, circles, upward triangles and downward triangles) are plotted as a function of $\tilde{n}/n_0$ with the first seven theoretically calculated modes (lines).

tional mode appears at V_{SG}=−1.9 V. Mapping of plasmon modes measured from 180 to 600 GHz in Fig. 2(b) demonstrates that the modes shown in Fig. 2(a) correspond to the second, third, and fourth excited modes. These plasma resonances are similar to those observed by Kang *et al.* in the 1–10 GHz range for HEMTs with wider gates at commensurate carrier densities that consequently result in sub-THz resonant frequencies.[17,18] The fundamental mode is at approximately 240 GHz with V_{SG}=0 V. Plasmonic modes are plotted as a function of $\tilde{n}/n_0$ where $\tilde{n}$ is the equilibrium 2D electron gas (2DEG) density under the SG and n_0 is the ungated 2DEG density. The 2DEG density below the SG is calculated assuming a capacitive coupling between gate and channel where $\tilde{n}=n_0(V_{TH}-V_{SG})/V_{TH}$.

To describe the cavity plasma oscillations in the partially gated cavity formed between the source contact and the BG we use the hydrodynamic model of a 2DEG which includes the Euler and continuity equations together with the Poisson equation for self-consistent electric potential ϕ in the plasma wave,[19]

$$\frac{\partial \delta v}{\partial t} + \delta v \frac{\partial v}{\partial x} = \frac{e}{m^*}\frac{\partial \phi}{\partial x} \quad \text{and} \quad \frac{\partial n}{\partial t} + \frac{\partial (n\delta v)}{\partial x} = 0, \tag{1}$$

$$\nabla^2_{x,z}\phi = \frac{e\delta n}{\varepsilon\varepsilon_0}\delta(z). \tag{2}$$

Here, $\delta n(x)$ and $\delta v(x)$ are fluctuations of the electron density and average velocity; $n=n_{eq}+\delta n$, where n_{eq} is an equilibrium 2DEG density (different in gated and ungated regions), and x and z axes are chosen in the source-drain direction and perpendicular to the 2D channel plane, respectively. At a given frequency ω, linearized solutions of Eqs. (1) and (2) can be found for both gated and ungated regions of the cavity. In these calculations we neglect damping of the electron density fluctuations due to scattering and also screening of the plasma oscillations in the gated regions because the 2DEG is sufficiently distant from the gate metallization. This latter approximation is more accurate for higher order modes. To find the plasmon dispersion law and distribution of electron density in the cavity plasma wave we used boundary conditions $\delta n(0)=0$ and $\delta v(L)=0$, where L is the distance between the source and the BG. These boundary conditions correspond to the zero density fluctuation at the grounded Ohmic source contact and zero drift current density at the BG where the channel is completely depleted.[20–22] Spatial distribution of the electric potential in the plasma wave in the narrow region near the boundary between the gated and ungated parts of the cavity has a complicated structure due to different equilibrium 2D electron density on the opposite sides of the boundary. Instead of calculating the details of the electric potential distribution in this region we have invoked *ad-hoc* hydrodynamic boundary conditions and assumed the continuity of $\delta n(x)$ and plasma current density $en_{eq}\delta v(x)$ at this boundary. The seven lowest plasma frequencies found within this model are plotted in Fig. 2(b) together with the experimental data as a function of $\tilde{n}/n_0$. Results in Fig. 2(b) were found for L=6 μm and $n_0=4.2\times10^{11}$ cm^{-2}. With no electron density modulation, i.e., V_{SG}=0 ($\tilde{n}=n_0$), 2D plasma resonances occur at the following:

$$\omega_m = \sqrt{\frac{\pi e^2 n_0 (2m-1)}{4m^*\varepsilon\varepsilon_0 L}} \quad m=1,2,\ldots, \tag{3}$$

and coincide with the plasma frequencies found in Ref. 20. In the strong modulation limit, $\tilde{n}/n_0 \ll 1$, plasma frequencies approach the value of,

$$\omega_m = \sqrt{\frac{3\pi e^2 \tilde{n} m}{2m^*\varepsilon\varepsilon_0 L}} \quad m=1,2,\ldots. \tag{4}$$

By examining the spatial distribution, $\delta n(x)$, we determine that the frequencies in Eq. (4) describe plasmon modes localized under the SG. There is excellent agreement between the fundamental mode in both experiment and model calculations. However, fewer higher order modes are seen experimentally than theoretically. We hypothesize that the coupling to certain modes is too weak to be seen in the pulsed source experiments.

Optimized detector sensitivity has been characterized using a continuous wave (CW) submillimeter source based on a series of Schottky multipliers designed by Virginia Diodes Inc.. The detector is biased utilizing the same scheme as in the pulsed experiments with FEL but the signal is measured using standard lock-in techniques by chopping the CW source. A second sample with identical design and operation was used for the CW characterization. Figure 3(a) illustrates the square law response of the detector over three orders of magnitude of incident power with 270 GHz excitation and 200 Hz modulation at T=20 K, I_{SD}=200 nA, and V_{BG}=−2.55 V. To within experimental error the response is a linear function of incident power. Under the same conditions the modulation frequency may be swept as shown in the inset of Fig. 3(a). The signal roll off at high modulation frequency is determined by the detector time constant. A detector time constant of 1.7 ms, corresponding to a cutoff frequency of 600 Hz, is consistent with time constant measurements from pulsed experiments and is in fact an "RC"

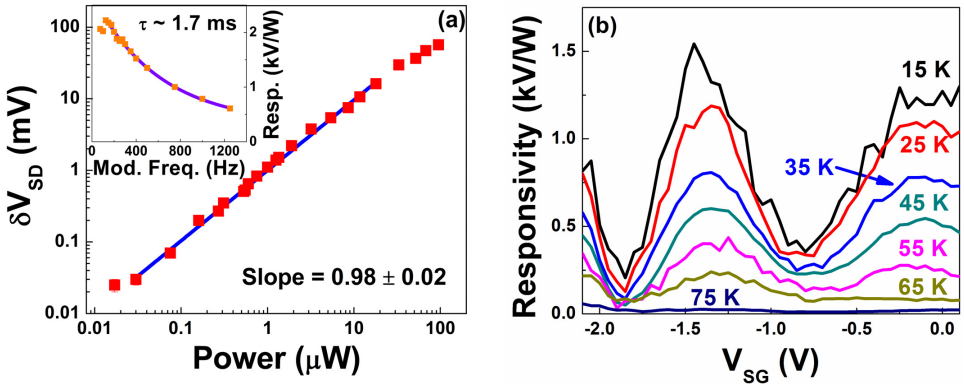

FIG. 3. (Color online) (a) Detector square law response under 270 GHz excitation with 200 Hz modulation at T=20 K, I_{SD}=200 nA, and V_{BG}=−2.55 V. The inset demonstrates roll-off in detector response with modulation frequency corresponding to a 1.7 ms time constant. (b) Resonant detector response from T=15 K to T=75 K under 270 GHz excitation and 200 Hz modulation with I_{SD}=200 nA and V_{BG}=−2.55 V.

circuit time constant.[13] Figure 3(b) shows the resonant response at 270 GHz as the detector temperature is increased. The resonant features remain evident up to 75 K; the width of the resonances does not appear to change appreciably. The width is not limited by mobility but most likely by radiation damping mediated by the coupling of the plasmon cavity to free space by the antenna. It is important to note that the responsivity only falls by a factor of four at 55 K, despite the fact that no effort was made to optimize the detector operating point at elevated temperatures.

The noise equivalent power (NEP) has been measured for detectors with both pulsed and modulated CW sources at 20 K. Using a pulsed source, we measured a responsivity of 2.5 kV/W with 240 GHz excitation. We calculate from this responsivity an optimal NEP of 4.6×10^{-10} W/Hz$^{1/2}$ based on noise density measurements with 150 Hz modulation. For CW experiments performed on a second sample, the optimal NEP was 5.4×10^{-10} W/Hz$^{1/2}$ with 236.5 GHz excitation and 750 Hz modulation. The peak responsivity measured was 6.7 kV/W. Both demonstrate sub-nW/Hz$^{1/2}$ NEPs and responsivities well above 1 kV/W at approximately the same excitation frequency corresponding to the fundamental 2D plasmon mode. With an additional improvement of two to three orders of magnitude in the NEP while maintaining the 1.7 ms time constant, the antenna coupled, 2D plasmonic cavity with bolometric sensor is an excellent candidate for real-time, narrowband, tunable THz imaging.

The authors would like to thank Dave Enyeart and Gerry Ramian for their assistance, maintenance and operation of the UCSB FEL facility. This work is supported by the University of Buffalo NSF-NIRT THz Collaboratory, Grant No. ECS0609146. This work was performed, in part, at the Center for Integrated Nanotechnologies, a U.S. Department of Energy, Office of Basic Energy Sciences user facility. Sandia National Laboratories is a multiprogram laboratory operated by Sandia Corporation, a Lockheed-Martin Co., for the U.S. Department of Energy under Contract No. DE-AC04-94AL85000. This material is based upon work supported by the U.S. Air Force Office of Scientific Research, Arlington, VA under Contract No. FA9550-09-C-0168 and Physical Sciences Inc. Andover, MA under Agreement No. FI011090528. Any opinions, findings and conclusions or recommendations expressed in this material are those of the author(s) and do not necessarily reflect the views of the U.S. AFOSR or Physical Sciences Inc.

[1]E. R. Brown, A. C. Young, J. Zimmerman, H. Kazemi, and A. C. Gossard, IEEE Microw. Mag. **8**, 54 (2007).
[2]M. Dyakonov and M. S. Shur, IEEE Trans. Electron Devices **43**, 380 (1996).
[3]F. Teppe, D. Veksler, V. Y. Kachorovski, P. Dmitriev, X. Xie, X. C. Zhang, S. Rumyantsev, W. Knap, and M. S. Shur, Appl. Phys. Lett. **87**, 022102 (2005).
[4]S. Kim, J. D. Zimmerman, P. Focardi, A. C. Gossard, D. H. Wu, and M. S. Sherwin, Appl. Phys. Lett. **92**, 253508 (2008).
[5]J. W. Song, N. A. Kabir, Y. Kawano, K. Ishibashi, G. R. Aizin, L. Mourokh, J. L. Reno, A. G. Markelz, and J. P. Bird, Appl. Phys. Lett. **92**, 223115 (2008).
[6]A. Lisauskas, U. Pfeiffer, E. Öjefors, P. H. Bolìvar, D. Glaab, and H. G. Roskos, J. Appl. Phys. **105**, 114511 (2009).
[7]S. J. Allen, D. C. Tsui, and R. A. Logan, Phys. Rev. Lett. **38**, 980 (1977).
[8]D. C. Tsui, E. Gornik, and R. A. Logan, Solid State Commun. **35**, 875 (1980).
[9]X. G. Peralta, S. J. Allen, M. C. Wanke, N. E. Harff, J. A. Simmons, M. P. Lilly, J. L. Reno, P. J. Burke, and J. P. Eisenstein, Appl. Phys. Lett. **81**, 1627 (2002).
[10]V. V. Popov, O. V. Polischuk, T. V. Teperik, X. G. Peralta, S. J. Allen, N. J. M. Horing, and M. C. Wanke, J. Appl. Phys. **94**, 3556 (2003).
[11]E. A. Shaner, M. Lee, M. C. Wanke, A. D. Grine, J. L. Reno, and S. J. Allen, Appl. Phys. Lett. **87**, 193507 (2005).
[12]E. A. Shaner, A. D. Grine, M. C. Wanke, M. Lee, J. L. Reno, and S. J. Allen, IEEE Photonics Technol. Lett. **18**, 1925 (2006).
[13]G. C. Dyer, J. D. Crossno, G. R. Aizin, E. A. Shaner, M. C. Wanke, J. L. Reno, and S. J. Allen, J. Phys.: Condens. Matter **21**, 195803 (2009).
[14]E. A. Shaner, M. C. Wanke, A. D. Grine, S. K. Lyo, J. L. Reno, and S. J. Allen, Appl. Phys. Lett. **90**, 181127 (2007).
[15]W. Knap, M. Dyakonov, D. Coquillat, F. Teppe, N. Dyakonova, J. Łusakowski, K. Karpierz, M. Sakowicz, G. Valusis, D. Seliuta, I. Kasalynas, A. El Fatimy, Y. M. Meziani, and T. Otsuji J. Infrared Milli. THz. Waves **30**, 1319 (2009), and references therein.
[16]V. Ryzhii, A. Satou, T. Otsuji, and M. S. Shur, J. Appl. Phys. **103**, 014504 (2008).
[17]P. J. Burke, I. B. Spielman, J. P. Eisenstein, L. N. Pfeiffer, and K. W. West, Appl. Phys. Lett. **76**, 745 (2000).
[18]S. Kang, P. J. Burke, L. N. Pfeiffer, and K. W. West, Appl. Phys. Lett. **89**, 213512 (2006).
[19]M. Dyakonov and M. S. Shur, Phys. Rev. Lett. **71**, 2465 (1993).
[20]M. Dyakonov and M. S. Shur, Appl. Phys. Lett. **87**, 111501 (2005).
[21]V. Ryzhii, A. Satou, and M. S. Shur, J. Appl. Phys. **93**, 10041 (2003).
[22]V. Ryzhii, A. Satou, I. Khmyrova, A. V. Chaplik, and M. S. Shur, J. Appl. Phys. **96**, 7625 (2004).